Structural decomposition of the chemical shielding tensor: Contributions to the asymmetry, anisotropy, and orientation

Judith Herzfeld,[a] Donald J. Olbris, Efim Furman, and Vadim Benderskiy
Department of Chemistry, MS #015, Brandeis University, Waltham, Massachusetts 02454-9110

(Received 1 May 2000; accepted 7 July 2000)

The nine elements of chemical shielding tensors contain important information about local structure, but the extraction of that information is difficult. Here we explore a semiempirical method that has the potential for providing relatively accessible structural correlations. The approach entails approximating the field-induced electron current density as entirely perpendicular to the applied field. This has two interesting consequences. (1) The resulting shielding tensor is perfectly symmetric. Thus, asymmetry in a shielding tensor is an indication of current density that is not orthogonal to the applied field. (2) The orientation dependence of the chemical shielding at a point of interest is related explicitly to the isotropic average of the chemical shielding at every point in the surrounding region. This suggests a relatively simple relationship between the orientation dependence of the chemical shielding and the molecular structure. Good correlation with experimental tensors is obtained with just one or two adjustable parameters in several series of compounds, including silicates, phosphates, hydrogen bonds, carboxyls, and amides. As expected, the results indicate that for a given center, the contribution to the shielding anisotropy that is associated with each bonded neighbor increases as the number of electrons at either the center or the neighbors increases. © *2000 American Institute of Physics.* [S0021-9606(00)31837-2]

I. INTRODUCTION

The power of nuclear magnetic resonance (NMR) is owed primarily to the electron currents induced around a nucleus by the applied magnetic field. Because these electron currents depend sensitively on local molecular structure, they carry chemical information. The degree to which the resulting secondary field opposes the applied field is known as the ''chemical shielding.'' The experimental consequence is an adjustment of the frequency of the magnetic resonance of the nucleus, known as the ''chemical shift.'' Since the electron currents depend on the orientation of the molecule in the magnetic field, the chemical shielding also depends on orientation. This variation is described by a second rank Cartesian tensor.

In the main, there have been two approaches to the interpretation of chemical shifts. The older method is strictly empirical: a family of related compounds is studied so that the variations of the chemical shift can be correlated with variations in structure. With increases in computational power and improvements in quantum methodology, *ab initio* calculations of chemical shifts have also become useful.

Maximum experimental information is obtained by examination of molecules in the solid state. When single crystals are available, spectroscopy and diffraction combined allow the nine elements of the full chemical shielding tensor $\vec{\sigma}$ to be specified in the molecular frame. However, the shielding asymmetry $(\vec{\sigma}-\vec{\sigma}^T)/2$ does not contribute to NMR spectra to first order and is neglected in most experiments. Thus single crystal studies generally report the six elements of the symmetric shielding tensor $(\vec{\sigma}+\vec{\sigma}^T)/2$. When only powders are available, only the three principal values of the symmetric shielding tensor can be obtained, with no orientation information. (For static samples, the principal values are obtained from the discontinuities in the powder pattern. For samples spinning at the magic angle, the principal values are derived from the intensities of the spinning sidebands.) From solution samples, only the isotropic average of the shielding can be measured. This scalar corresponds to one third of the trace of the full tensor, $\sigma_{\mathrm{iso}}=Tr(\vec{\sigma})/3$.

Clearly the full shielding tensor carries the most information. It is also the most difficult to grasp intuitively and calculate *ab initio*. In the present work, we consider the utility of neglecting some of the field-induced electron current. We find that our simplification provides some qualitative and semiquantitative insights into the orientation dependence of the chemical shielding. In the following section, we introduce our approximation of the current and derive the shielding anisotropies under this approximation. In the succeeding section, a further numerical approximation connects the shielding anisotropy to molecular structure and allows comparisons with data for several families of compounds. The data analysis is followed by a discussion of the approach and results, and a summary of the conclusions.

II. APPROXIMATION OF THE FIELD INDUCED ELECTRON CURRENT

In an isolated atom, the electron current flows perpendicular to the applied field, following circular paths around the nucleus. This corresponds to a reduction of the spherical symmetry of the isolated atom to cylindrical symmetry in the presence of the magnetic field. In the presence of additional nuclei, the field-induced circulation of the electrons is much more complicated. Therein lies the power and the difficulty. Although the electron flow in polyatomic molecules is not circular, much of the current is in the plane perpendicular to

[a]Author to whom correspondence should be addressed.

the applied field. In the present work, we examine the results of assuming that the current that is not perpendicular to the applied field can be neglected.

Conservation of charge requires that the electron current density $\mathbf{j}(\mathbf{r})$ be divergenceless. If we also assume that the current is entirely perpendicular to the applied magnetic field $\mathbf{B}$, then the current in the linear response regime must take the form

$$\mathbf{j}(\mathbf{r}) = \nabla f(\mathbf{r}) \times \mathbf{B}, \tag{1}$$

where $f(\mathbf{r})$ is an unknown well-behaved function. This current makes its own contribution to the magnetic field

$$\mathbf{B}'(\mathbf{R}) = -\frac{1}{c}\int \frac{(\mathbf{r}-\mathbf{R})\times\mathbf{j}(\mathbf{r})}{|\mathbf{r}-\mathbf{R}|^3} d\mathbf{r}, \tag{2}$$

which causes the effective magnetic field at any given location to be different from the applied field.

The chemical shielding tensor $\vec{\vec{\sigma}}(\mathbf{R})$ summarizes the relationship between the applied and induced fields

$$\mathbf{B}'(\mathbf{R}) = -\vec{\vec{\sigma}}(\mathbf{R})\cdot\mathbf{B}. \tag{3}$$

By combining Eqs. (1)–(3) and integrating by parts, one finds that

$$\sigma_{ij}(\mathbf{R}) = \frac{1}{c}\int \left\{ \frac{\partial^2}{\partial r_i \partial r_j}\left(\frac{1}{|\mathbf{r}-\mathbf{R}|}\right) + 4\pi\delta(\mathbf{r}-\mathbf{R})\,\delta_{ij}\right\} f(\mathbf{r})\, d\mathbf{r}, \tag{4}$$

where δ_{ij} is the Kronecker delta function. The symmetry $\sigma_{ij}=\sigma_{ji}$ of Eq. (4) demonstrates that any asymmetry in chemical shielding tensors must be due to electron currents that are not orthogonal to the applied field.

For the isotropic average of the chemical shielding, Eq. (4) gives

$$\sigma_{\mathrm{iso}}(\mathbf{R}) = \sum_i \frac{\sigma_{ii}(\mathbf{R})}{3} = \frac{8\pi}{3c} f(\mathbf{R}). \tag{5}$$

Combining Eqs. (4) and (5) then gives

$$\sigma_{ij}(\mathbf{R}) - \sigma_{\mathrm{iso}}(\mathbf{R})\,\delta_{ij} = \int \left\{ \frac{(\mathbf{r}-\mathbf{R})_i(\mathbf{r}-\mathbf{R})_j}{|\mathbf{r}-\mathbf{R}|^5} - \frac{\delta_{ij}}{3|\mathbf{r}-\mathbf{R}|^3}\right\} \frac{9\sigma_{\mathrm{iso}}(\mathbf{r})}{8\pi} d\mathbf{r}. \tag{6}$$

Thus if the field-induced electron current is entirely perpendicular to the applied field, the anisotropy $(\sigma_{ij}-\sigma_{\mathrm{iso}}\delta_{ij})$ of the shielding (i.e., the deviation of the chemical shielding at a given point from the isotropic average at that point) is directly related to the variation of the isotropic average of the shielding in the surrounding space.

III. STRUCTURAL DECOMPOSITION

While the result of Eq. (6) is conceptually interesting, it is of no practical value. However, a useful semi-empirical expression might be obtained if the spatial integral can be approximated by a sum over a few points,

$$\sigma_{ij}(\mathbf{R}) - \sigma_{\mathrm{iso}}(\mathbf{R})\,\delta_{ij} = \sum_N \left\{ \frac{(\mathbf{R}_N-\mathbf{R})_i(\mathbf{R}_N-\mathbf{R})_j}{|\mathbf{R}_N-\mathbf{R}|^5} - \frac{\delta_{ij}}{3|\mathbf{R}_N-\mathbf{R}|^3}\right\} S_N. \tag{7}$$

Here S_N is a weighting factor for the Nth point that takes into account the isotropic shielding over the volume that the point represents.

The sum that first comes to mind is over nearest neighbor atoms. This has two virtues. First the positions of these points are directly related to molecular structure. Thus, the anisotropy of the shielding might be given explicitly in terms of the orientations and lengths of chemical bonds. It is also the case that extrema of σ_{iso} are expected at nuclear centers[1] and therefore summing at those points would be particularly efficient. In the following section, we test the usefulness of the sum over atoms in a variety of systems.

IV. DATA ANALYSIS

In order to determine how well Eq. (7) connects the chemical shift anisotropy to the molecular structure, it is necessary to have access to both. Compounds were therefore selected for which both crystallographic and solid state NMR data are available. The compounds and the corresponding sources of the data are listed in the supplementary material.[2]

The nine elements of the tensor described by Eq. (7) represent only five independent variables because the tensor is symmetric and traceless. Comparison of the results with experimental data requires diagonalizing the tensor to obtain the three principle values, $(\sigma_{ii}-\sigma_{\mathrm{iso}})$ for $i=1,2,3$ (of which only two are independent because the tensor is traceless) and the three angles that specify the orientation of the principle axis system.

The sum over neighboring atoms in Eq. (7) may be further simplified if the weighting factor S_N is the same for all of the bonded atoms. In this case, the weight is a constant multiplicative factor for all the terms in Eq. (7). Its magnitude scales the principal values of the tensor and its sign determines, in binary fashion, which directions are the least and most shielded. This single weight description is where we begin our analysis of the efficacy of Eq. (7). Thereafter, we consider more complicated cases with multiple weights.

A. Single weight

The single weight approximation is most reasonable if the neighboring atoms are all of the same element and we restrict this section to such systems. We begin with octahedral systems, in which the atomic positions cover the surrounding space relatively densely. We then proceed to sparser systems, for which the sum over atoms discretizes the integral in Eq. (6) more coarsely.

Figure 1 shows the results for vanadium shielding anisotropies $(\sigma_{ii}-\sigma_{\mathrm{iso}})$ in octahedral vanadate centers. The correspondence between the experimentally measured values and the values calculated from crystals structures was obtained from the least-squares fit of a single weighting factor that is the same for all the oxygen atoms. Clearly Eq. (7), with just one adjustable parameter (S_0), captures much of the variation in the anisotropy, in spite of the various as-

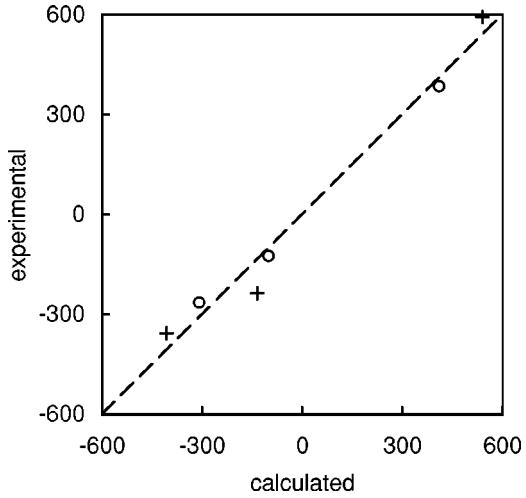

FIG. 1. Correlation for ^{51}V in approximately octahedral vanadates. Experimentally determined values of $\sigma_{ii}-\sigma_{iso}$ (in ppm) vs the values from the structure-based calculation [Eq. (7)] (in ppm). + represents data from single crystals and ○ qrepresents data obtained from powders. Perfect agreement between the experimental and calculated values is represented by the diagonal line. For the best fit shown here $S_0=14\,100$ ppm Å^3 and the RMSD=56 ppm=5.9% of the overall variation.

sumptions made in the calculation (i.e., electron currents orthogonal to the field, sum over atoms, and equivalence of the oxygen weights). The residual root mean square deviation (RMSD) between the calculated values and the experimental values is 56 ppm which is only 5.9% of the full range of variation.

The one single crystal NMR study for octahedral vanadates also allows us to check our predictions for the tensor orientation. As shown in Table I, the orientations of the eigenvectors are predicted quite accurately using Eq. (7) with the positive sign for S_0 obtained from the best fit of the eigenvalues.

Figure 2 shows the correlations that we obtain between experimental and calculated anisotropies for a variety of tetrahedral centers. For each class of compounds we have again assumed a single weight for all the neighboring atoms which has the effect of acting as a simple scaling factor for the calculation. In these cases, Eq. (7) taken as a sum over nearest neighbor atoms can account for the variation in the tensor elements with a RMSD that is only 8%–11% of the full range. The correlation for the silicates is similar to that for the octahedral vanadates, while the correlation is less good for the other tetrahedral systems. What the octahedral vanadates and the tetrahedral silicates have in common is sp^3 oxygen atoms. In contrast, the other tetrahedral systems have

TABLE I. Shielding tensor orientations for octahedral centers: ^{51}V in vanadates. Angles between the calculated and experimental eigenvectors are given for the most shielded, least shielded and middle eigenvalues.

Compound	Most	Middle	Least
V_2O_5	3°[a]	3°[a]	0°

[a]Here we report the angle to the crystal axis. The corresponding experimental tensor directions are reported to lie within 1.5° of those axes. The least shielded direction, both calculated and measured, is constrained by symmetry to lie along the third crystal axis.

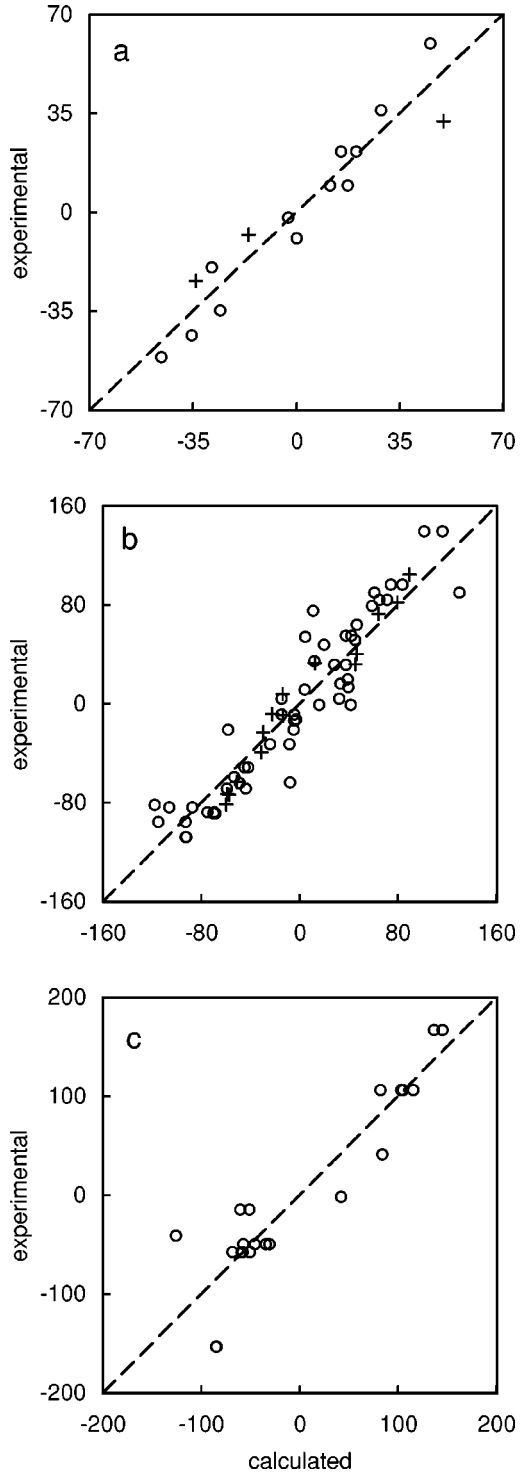

FIG. 2. Correlations for tetrahedral centers. Best fits for (a) ^{29}Si in silicates ($S_0=855$ ppm Å^3 and RMSD=8.9 ppm=8.0%); (b) ^{31}P in phosphates ($S_0=957$ ppm Å^3 and RMSD=23.7 ppm=9.6%); and (c) ^{31}P in phosphorus sulfides ($S_S=4050$ ppm Å^3 and RMSD=35.7 ppm=11%). Axes, symbols, and diagonal as in Fig. 1.

a varying mixtures of sp^3 and sp^2 neighbors for which the use of a single weight is expected to be less satisfactory.

Single crystal NMR studies are available for systems in two of the three tetrahedral classes of compounds. Tables II (silicates) and III (phosphates) show the comparisons of the eigenvector orientations determined experimentally with

TABLE II. Shielding tensor orientations for tetrahedral centers: ^{29}Si in silicates. Angles between the calculated and experimental eigenvectors are given for the most shielded, least shielded and middle eigenvalues.

Compound	Most	Middle	Least
Mg_2SiO_4 (A)	5°	0°	5°
Mg_2SiO_4 (B)	10°	0°	10°

those obtained from Eq. (7) using the signs of the weights obtained in the best fit of the eigenvalues. The accuracy is seen to be almost as good for the silicates as for the octahedral vanadates. For the phosphates the quantitative accuracy is less good, which is not surprising given the poorer correlation of the eigenvalues and the greater heterogeneity of oxygen neighbors as discussed above. However, the qualitative assignments of the directions of the eigenvectors is correct in all but one of the phosphates.

Still sparser bonding occurs in the roughly linear system of a proton in a hydrogen bond. Figure 3 shows the correlations obtained for the shielding anisotropies of protons in O–H···O systems, again using a single weighting factor for the oxygen atoms. The data available are rather limited because the sensitivity of Eqs. (6) and (7) to the position of the hydrogen atom requires that we restrict our analysis to cases in which neutron diffraction data are available. Of course, it is also necessary to restrict the analysis to systems in which the proton does not exchange between multiple sites. However, even with the limited data set, we can see that although the integral of Eq. (6) has been reduced to a sum over just two points, the calculated anisotropies reflect the experimental variation in the tensor elements with a RMSD that is only 11% of the full range. This is similar to the correlations obtained for systems with mixtures of sp^3 and sp^2 oxygens.

Closer examination of Fig. 3 also shows that both theory and experiment find the unique direction (along the hydrogen bond) to be the most shielded. A quantitative comparison of the experimental and theoretical tensor orientations is shown in Table IV. The theory accurately predicts the orientation of the most shielded element. For the other elements, poorer accuracy is due to near axial symmetry of the arrangement of the atoms included in the calculation.

TABLE III. Shielding tensor orientations for tetrahedral centers: ^{31}P in phosphates. Angles between the calculated and experimental eigenvectors are given for the most shielded, least shielded and middle eigenvalues.

Compound	Most	Middle	Least
$Ba[(C_2H_5O)_2PO_2]_2$	12°	8°	10°
deoxycytidine 5′-monophosphate	18°	22°	20°
$NH_3CH_2CH_2OPO_3H$	8°[a]	30°[a]	31°[a]
$K_2(C_6H_{11}O_5)OPO_3\cdot 2H_2O$	21°	17°	19°
$CO(NH_2)_2\cdot H_3PO_4$	47°	60°	79°

[a]These relative angles are more approximate than the others because the experimental angles were read by eye from a figure in the NMR paper: the ellipsoids in the figure appeared to align with bonds, and with planes defined by pairs of bonds, the directions of which could be calculated from the atomic position data.

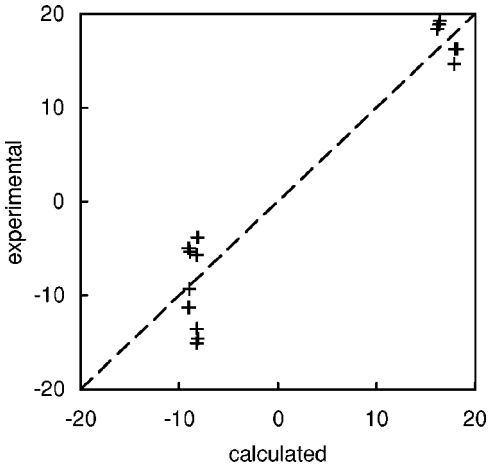

FIG. 3. Correlations for protons in hydrogen bonds between two oxygen atoms. Axes, symbols and diagonal as in Fig. 1. For the best fit shown here $S_0=22.8$ ppm Å^3 and RMSD=3.8 ppm=11%.

B. Two weights, one set to zero

In the foregoing cases, single parameter descriptions were based on identical weights for all of the neighboring atoms. A single parameter description can also be appropriate when there are two types of neighboring atoms if the weight for one type is negligible compared to that of the other. Negligible weights may apply for hydrogen atoms. In HCN, for example, the isotropic shielding has peaks at the carbon and nitrogen, but not at the hydrogen.[1]

Figure 4 shows the eigenvalue correlations that we obtain for tetrahedral carbon atoms with varying numbers of carbon and hydrogen neighbors when no weight is assigned to the hydrogens and a single weight for the carbons is varied to obtain the best fit. Although there is considerable scatter, there is no systematic deviation and the experimental variation of the eigenvalues is accounted for with a RMSD that is only 10% of the full range. Furthermore, the principal axes from single crystal NMR studies are well reproduced, as shown in Table V. A qualitative misassignment of tensor orientation occurs only for one of the compounds. This compound has one of the smaller anisotropies, which makes the

TABLE IV. Shielding tensor orientations for linear centers: ^{1}H and ^{2}H in O–H···O hydrogen-bonds. Angles between the calculated and experimental eigenvectors are given for the most shielded, least shielded, and middle eigenvalues.

Compound	Most	Middle	Least
$KH[O(CH_2COO)_2]$	10°	20°	18°
$KH[CH_2(COO)_2]$	9°	a	a
$KH[CH_3(CH)_2COO]_2$	1°	53°[b]	53°[b]
squaric acid[c] (A)	3°	3°	0°
squaric acid[c] (B)	3°	3°	0°
$(NH_4)H(COO)_2\cdot\frac{1}{2}H_2O$	2°	50°[b]	50°[b]

[a]No unique angle between the calculated and experimental results can be reported because the calculated eigenvalues are degenerate, and the corresponding eigenvectors are only determined to a plane.

[b]The angles are probably meaningless because the calculated eigenvalues are nearly degenerate and the corresponding eigenvectors are therefore probably only determined to a plane.

[c]3,4-dihydroxy-3-cyclobutene-1,2-dione.

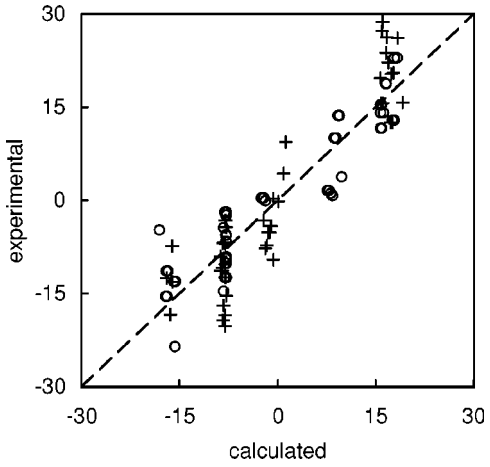

FIG. 4. Correlations for ^{13}C in tetrahedral centers with proton and carbon neighbors, assuming $S_H=0$. Axes, symbols, and diagonal as in Fig. 1. For the best fit shown here $S_C=84.8$ ppm Å^3 and RMSD=5.2 ppm=10%.

distinctions between directions less clear cut. However, given the accurate prediction of the orientation of another tensor of comparable span and another even narrower tensor, we consider it possible that the misassigned case is due to problems with the experimental report. Otherwise, experiment and theory (with the positive weight for carbon) agree that the unique axis in the methyl groups is most shielded and the unique axis in the methylidyne groups is the least shielded. In the methylene groups, the least shielded direction is along the vector connecting the two protons and the most shielded is along the vector connecting the two carbon neighbors.

Since Fig. 4 includes quite a variety of carbon centers, the scatter can be due to several factors. One may be the neglect of the hydrogen atoms. The various panels of Fig. 5 show the same correlations as in Fig. 4 separated according to the number of hydrogen neighbors around the central carbon. Since the scatter seems to be similar in all groups, the neglect of protons does not seem to be a factor. However, it is now more clearly apparent that shieldings that are computed as closely similar in the theory (horizontal axis) are found to be rather dispersed in experiments (vertical axis). Whatever these variations are, they are not reflected in the positions of the neighbors that go into the calculation. This suggests that they have to do with the chemical character of the neighbors. Indeed, the bonding of the nearest neighbors to second nearest neighbors varies considerably. It includes polar as well as nonpolar bonds, and double bonds as well as single bonds. These variations are probably the source of much of the vertical dispersion in Fig. 5.

TABLE V. Shielding tensor orientations for tetrahedral centers: ^{13}C with varying numbers of carbon and hydrogen neighbors as indicated. Angles between the calculated and experimental eigenvectors are given for the most shielded, least shielded and middle eigenvalues.

Compound	Most	Middle	Least
4 C, 0 H neighbors			
dimedone[b]	4°	22°	21°
$C(CH_3)_2(COOH)_2$	42°	90°	89°
2 C, 2 H neighbors			
Meldrum's acid[c]	3°	9°	8°
hexaethyl benzene	15°	15°	2°
L-asparagine monohydrate	1°	8°	8°
1 C, 3 H neighbors			
Meldrum's acid[c] (A)	3°	a	a
Meldrum's acid[c] (B)	3°	a	a
dimedone[b] (A)	4°	a	a
dimedone[b] (B)	3°	a	a
hexaethyl benzene	20°	a	a
1,1,2,2-tetraacetylethane (A)	11°	a	a
1,1,2,2-tetraacetylethane (B)	2°	a	a
$C(CH_3)_2(COOH)_2$	3°	a	a

[a]No unique angle between the calculated and experimental results can be reported because the calculated eigenvalues are degenerate, and the corresponding eigenvectors are only determined to a plane.
[b]5,5-dimethylcyclohexane-1,3-dione.
[c]2,2-dimethyl-1,3-dioxane-4,6-dione.

C. Multiple weights

For centers with heterogeneous neighbors, multiple weights are expected to provide a more satisfactory description. A relatively simple case is provided by the carbon center of the guanidyl group of arginine. This carbon has three nitrogen neighbors, two of which are terminal nitrogens (the η nitrogens) and one of which connects the group to the sidechain (the δ nitrogen). Figure 6(a) shows the best fit for the carbon chemical shielding when all three nitrogen neighbors are assigned the same weight. Instead of scatter, one finds a systematic deviation because all the arginine compounds are very similar. One also finds mixed tensor orientations. When different weights are used for the two classes of nitrogen neighbors, the correlation is much improved and the tensor orientation is consistent. However, with various pairs of weights, good fits are obtained for all six possible tensor orientations relative to the two planes of (near) molecular symmetry. Figures 6(b) and 6(c), show the two best fits, both of which assign the most shielded tensor element close to the direction of the $\delta-\epsilon$ bond. However, the other four fits have RMSD only about 20% larger. The fact that the two weights for the nitrogens are underdetermined by the data at hand is due to the similarity of the guanidyl groups in the arginine residues. Because the data are tightly clustered, we are effectively fitting just two points (the third being dependent on the other two) with two weights. For the weights to be properly determined requires a more varied set of compounds or experimental information on the orientation of the shielding tensor, neither of which is available for guanidyl nitrogens as far as we know.

Variability and orientation information are both available for carboxyl carbons. In this case, nonsense (i.e., a poor fit and incorrect tensor orientations) is obtained when a single weight is used for all three neighbors (two oxygens and one carbon). With different weights for the carbon and oxygen atoms, the best fit [Fig. 7(a)] shows good correlation and the correct tensor orientation for both the protonated and deprotonated carboxyl groups. However, this fit still treats the two oxygen atoms as identical to one another, a simplification that is more appropriate for deprotonated carboxyl groups than for protonated carboxyl groups. Figure 7(b) shows the improved fit for that orientation that is obtained

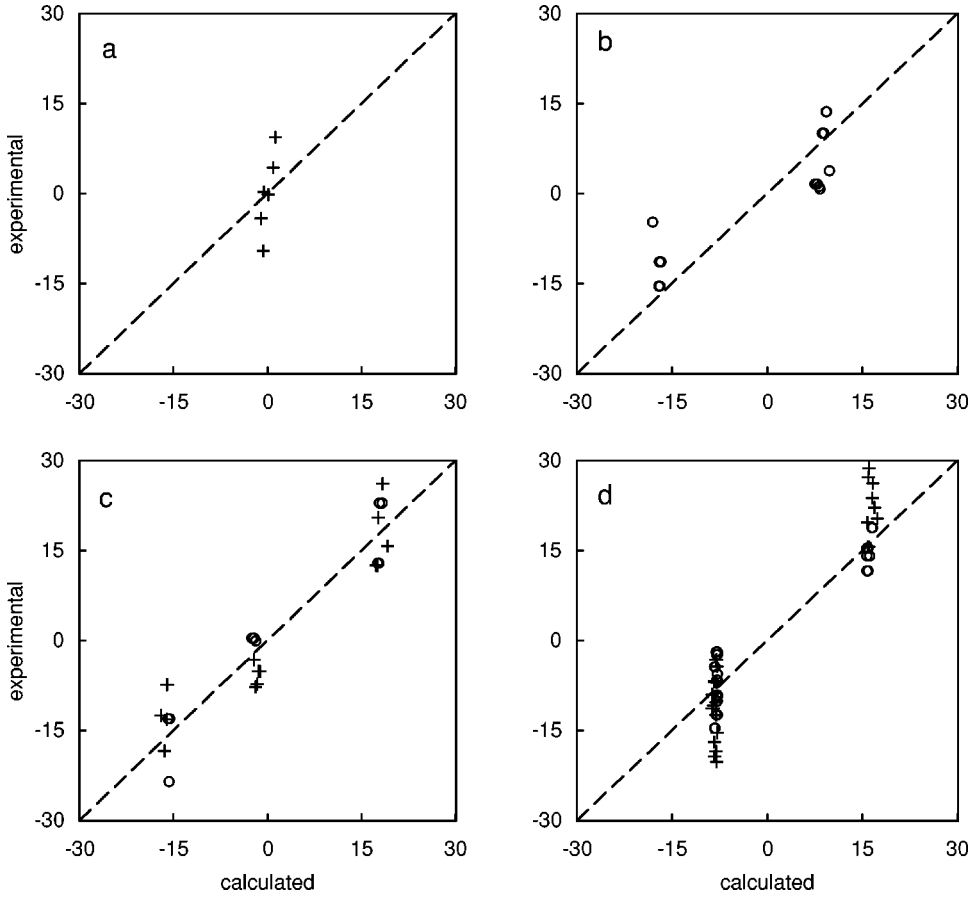

FIG. 5. Correlations for ^{13}C in tetrahedral centers with specific numbers of proton and carbon neighbors: (a) 4 carbon neighbors; (b) 3 carbon neighbors and 1 proton neighbor; (c) 2 carbon neighbors and 2 proton neighbors; and (d) 1 carbon neighbor and 3 proton neighbors. Axes, symbols, diagonal, and parameters as in Fig. 4.

for the deprotonated carboxyl groups alone. With the same carbon weight, an improved fit can also be obtained for the protonated carboxyls [Fig. 7(c)] by allowing two different weights for the oxygens. Consistent with the view of deprotonated carboxyl groups as resonance structures, the single oxygen weight obtained for the deprotonated carboxyl groups is close to the average of the two oxygen weights obtained for the protonated carboxyl groups.

In both the guanidyl and carboxyl cases, some of the weights are negative. This is expected due to low-lying electronic excitations which produce deshielding in the plane of the molecule. Such paramagnetic contributions are included in the spatial integral of Eq. (6) and the sum-over-points of Eq. (7). Having restricted the sum-over-points to a sum-over-atoms, we find the paramagnetic contribution absorbed in the weights for the atomic centers, shifting them to lower values.

D. Multiple weights with a paramagnetic dummy

An alternative is to treat the paramagnetic contribution explicitly. This is particularly advantageous in the case of the amides. For the nitrogen shielding tensor of amides, a description restricted to a sum-over-atoms requires the combination of a positive weight for the carbonyl carbon with negative weights for the other two atoms (whether carbon or hydrogen). The need for different carbon weights and nonzero hydrogen weights is clumsy. Both can be avoided by an explicit treatment of the paramagnetic contribution which is relatively simple in amides. This involves situation of a dummy atom along the axis perpendicular to the plane defined by the orbitals for the low-lying electronic transition. For the amide nitrogen this is in the amide plane, perpendicular to the amide bond. We arbitrarily place the dummy 1 Å from the nitrogen on this axis. Figure 8 shows the fit obtained for peptide nitrogens with the dummy carrying a negative (deshielding) weight, all the carbons carrying a single positive weight, and the protons assigned a zero weight. This two-parameter fit gives a good correlation [Fig. 8(a)] for a mixture of peptide nitrogens (including prolines where the proton is replaced by a third carbon), although a somewhat better fit is obtained when the proline and nonproline amides are fit separately [Figs. 8(b) and 8(c)]. This description also gives the correct orientation of the shielding tensor, with the middle element perpendicular to the amide plane. Finally, by addressing the paramagnetic effect separately, the weights obtained for the carbon neighbors are consistent with those found for carbon neighbors in systems without lowlying electronic transitions (Fig. 4).

V. DISCUSSION

In the present work, we have made the approximations that:

(1) the electron current induced by a magnetic field is orthogonal to the field;
(2) the integral of Eq. (6) can be replaced by a sum over neighboring atoms; and
(3) weights associated with summation on atoms of the same element are equal.

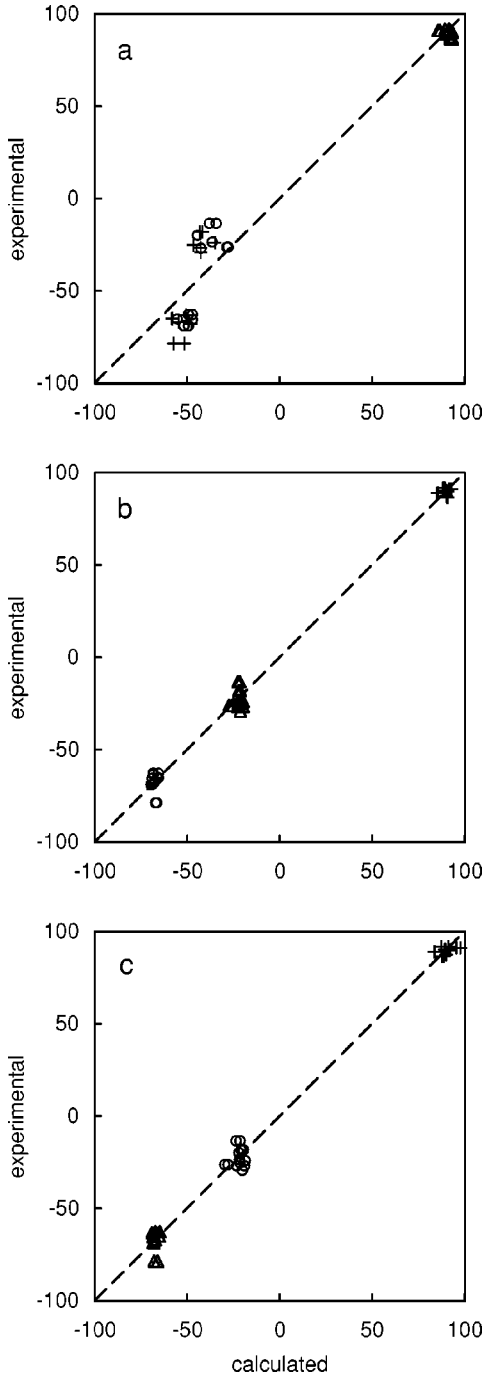

FIG. 6. Correlations for ^{13}C in the guanidyl group of arginine compounds. Axes and diagonal as in Fig. 1. Out-of-plane element=△, element closest to the $\delta-\epsilon$ bond = +, element orthogonal to the other two =○. (a) Best fits for a single nitrogen weight (a: with $S_N=-215$ ppm Å^3 and RMSD=14 ppm=8.4%) and two nitrogen weights (b: with $S_\delta=296$ ppm Å^3, $S_\eta=-72.1$ ppm Å^3, and RMSD=4.6 ppm=2.7%) and (c: with $S_\delta=330$ ppm Å^3, $S_\eta=71.9$ ppm Å^3, and RMSD=4.9 ppm=2.9%).

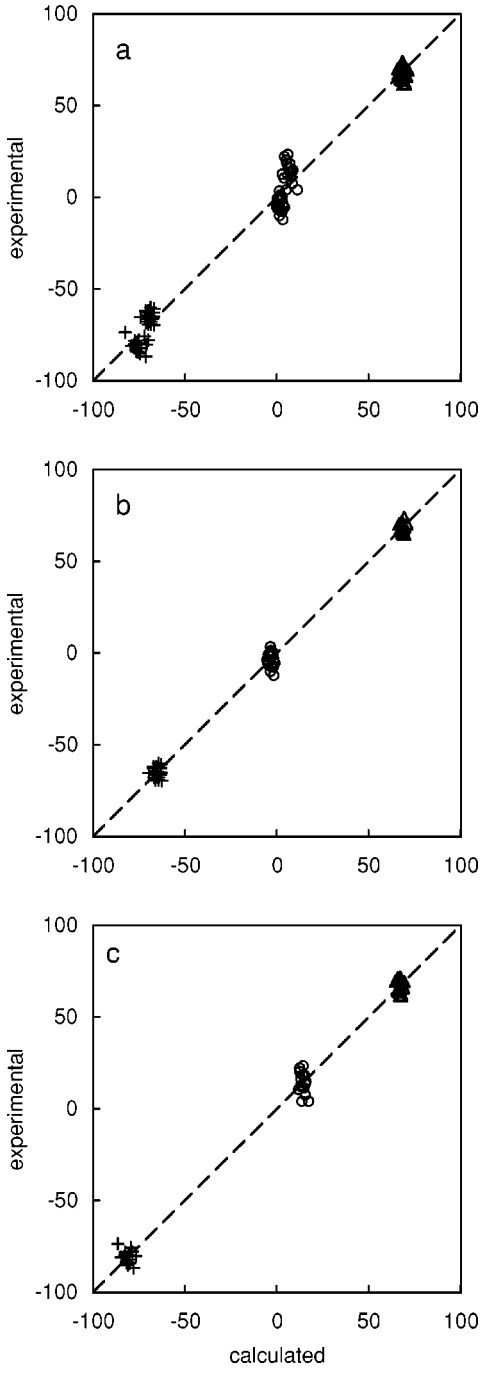

FIG. 7. Correlations for ^{13}C in carboxyl compounds. Axes and diagonal as in Fig. 1. Out-of-plane element =△, element closest to the bisector of the O–C–O angle = +, element orthogonal to the other two =○. (a) Protonated and deprotonated carboxyls (best fit $S_C=-431$ ppm Å^3, $S_0=-81.5$ ppm Å^3, and RMSD=6.3 ppm=3.9%). (b) Deprotonated carboxyls alone (best fit $S_C=-414$ ppm Å^3, $S_0=-88.7$ ppm Å^3, and RMSD =3.4 ppm=2.4%). (c) Protonated carboxyls alone (with fixed $S_C=-414$ ppm and best fit $S_{0'}=-34.6$ ppm Å^3, $S_{0''}=-117$ ppm Å^3, and RMSD=4.9 ppm=3.1%).

The first approximation has also been employed in some recent density functional work,[3] beginning with the observation that the most general form for a divergenceless electron current is

$$\mathbf{j}(\mathbf{r})=\nabla\times\mathbf{M}(\mathbf{r}), \tag{8a}$$

where, in the linear response regime,

$$\mathbf{M}(\mathbf{r})=M^{(0)}(\mathbf{r})\mathbf{B}+\mathbf{M}^{(1)}(\mathbf{r})\times\mathbf{B}+\vec{M}^{(2)}(\mathbf{r})\cdot\mathbf{B}. \tag{8b}$$

Since the symmetry of the susceptibility tensor dictates that $\mathbf{M}^{(1)}=0$, our neglect of currents that are not orthogonal to the applied field corresponds to assuming that $\vec{M}^{(2)}$ is negligibly small. This approximation was also taken in the early stages of development of the magnetic field density

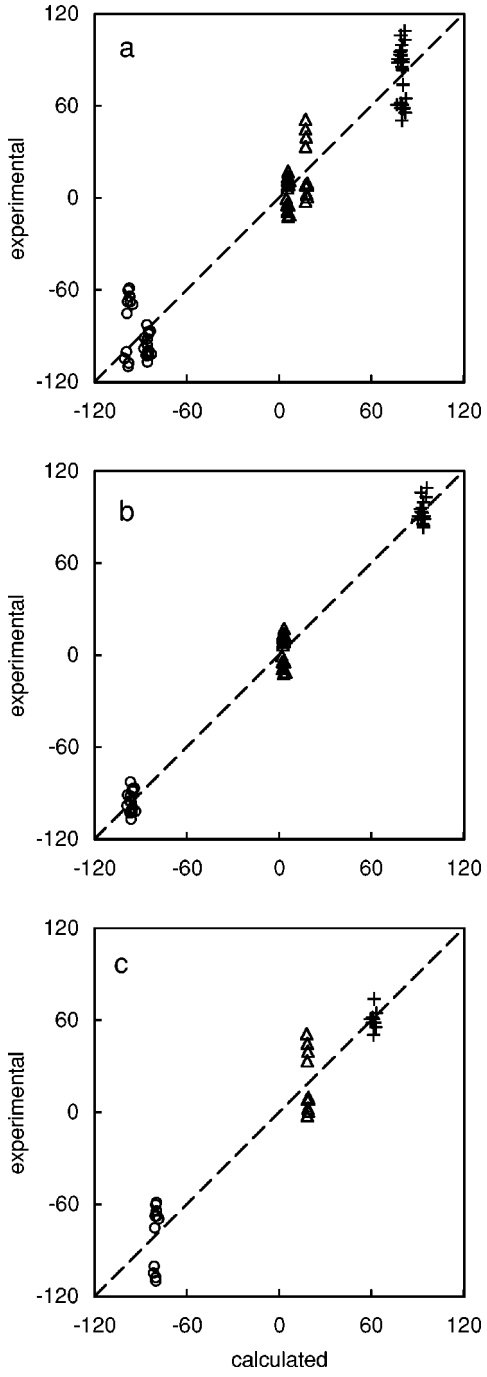

FIG. 8. Correlations for ^{15}N in amides. Axes and diagonal as in Fig. 1. Out-of-plane element $=\triangle$, element closest to the carbonyl–N bond $=+$, element orthogonal to the other two $=\bigcirc$. (a) Proline and nonproline amides (best fit $S_C=120$ ppm Å^3, $S_{\text{dummy}}=-143$ ppm Å^3, and RMSD=17 ppm =7.7%). (b) Proline amides alone (best fit $S_C=147$ ppm Å^3, $S_{\text{dummy}}=-163$ ppm Å^3, and RMSD=8.0 ppm=3.7%); and (c) Nonproline amides alone (best fit $S_C=82.7$ ppm Å^3, $S_{\text{dummy}}=-118$ ppm Å^3, and RMSD=16 ppm=8.7%).

functional theory.[3] The resulting local current density functional provided qualitative accuracy for the isotropic chemical shielding of hydrogen in some small molecules.[4] However, practical application to other elements was stymied by the divergence of electron density derivatives at the nuclear cusp.[5]

Our second approximation leads to a useful structural decomposition of the results of the first approximation. Taken as a sum over atoms, Eq. (7) construes the chemical shielding tensor as a sum of axially symmetric ''bond tensors,'' each with its unique axis oriented along a bond. Such a construction has previously been pursued on a strictly empirical basis specifically for the phosphorus shielding in phosphate compounds.[6] Scaling the P–O bond tensors linearly with bond order produced encouraging correlations with experimental values of $(\sigma_{ii}-\sigma_{\text{iso}})$ and the residual systematic deviations were attributed to the neglect of variations from tetrahedral bond angles. Our derivation of Eq. (7) provides a principled basis for adopting ''bond tensors'' and a quantitative framework for including variations of both bond lengths and bond angles.

The sum over atoms appears to be a robust way to discretize Eq. (6) for systems that do not have low-lying excited states. In these systems, we see that there is little erosion in the quality of the correlations between the theory and experiment as the discretization becomes coarser with decreasing numbers of neighbors. For these systems, the quality of the correlations seems to be primarily related to the limitations of our third approximation. As is to be expected, a single weight is not completely effective for chemically different neighbors, even if they are of the same element.

The limitations of our second approximation become evident in systems with low-lying electronic transitions. In these systems, there is paramagnetic shielding in the direction perpendicular to the plane defined by the orbitals involved in the transition. If these contributions are to be absorbed by atomic centers, the weights for the atoms must be skewed. At least in the case of the amides, we find that a simpler and more informative description can be had by adding a deshielded dummy atom to the sum over atoms. The weights for the neighboring carbons are then similar to those found in systems without low-lying electronic transitions.

Table VI compares the various weights found for different neighbors around different centers, each listed in order of increasing atomic number. As expected, the weights increase with increases in the number of electrons that each represents in the discretization of Eq. (6). The biggest jumps are between different rows of the Periodic Table.

TABLE VI. Summary of weights (in ppm Å^3) for least-squares fits of chemical shielding elements in systems with no low-lying electronic transitions (Figs. 1–4) and systems with low-lying transitions treated explicitly (Fig. 8).

	Neighbor			
Center	H	C	O	S
H			22.8	
C	~0[a]	84.8		
N	~0[a]	120[b]		
Si			855	
P			957	4050
V			14 100	

[a]The proton weight was not fit to the data. Approximation at zero gave good correlation with the experimental eigenvalues and eigenvectors of the chemical shielding.

[b]For proline and nonproline amides together. For the two groups separately, the best fit weights are 147 and 82.7, respectively (see Fig. 8).

VI. CONCLUSIONS

We have shown that several insights into the chemical shielding tensor can be obtained by approximating the field-induced electron current as entirely perpendicular to the field. First, we have shown that the resulting shielding tensor is exactly symmetric. Therefore any asymmetry in the shielding tensor is due to electron currents that are not orthogonal to the applied field. Symmetric tensors do not rule out nonorthogonal currents, but asymmetric tensors give unequivocal evidence for nonorthogonal currents.

We have also shown that the symmetric tensor that results from orthogonal electron currents has an anisotropy that is explicitly related to the variation of the isotropic average of the shielding in the surrounding space. This dependence takes a simple form and drops off as distance cubed.

Finally, we have developed a potentially useful variation of this relationship by assuming that the important contributions to the shielding anisotropy come primarily from the regions of the directly bonded neighbors. Using this relationship for several classes of compounds, we have shown that molecular structure can be used to predict much of the variation in the chemical shielding anisotropy with just one or two empirical parameters. For systems with low-lying electronic transitions, it is sometimes useful to treat the paramagnetic contribution explicitly by including a deshielded dummy neighbor.

ACKNOWLEDGMENTS

This work benefited from discussions with Alan E. Berger, Jining Han, Bruce Foxman, and Eric Kramer. The work was supported by NIH Grant No. GM 36810 and a Howard Hughes Medical Institute Summer research fellowship to E.F.

[1] K. Wolinski, J. Chem. Phys. **106**, 6061 (1997).
[2] See EPAPS Document No. E-JCPSA6-113-318037 for a complete list of compounds and data sources. This document file may be retrieved via the EPAPS homepage (http://www.aip.org/pubservs/epaps.html) or from ftp.aip.org in the directory /epaps/. See the EPAPS homepage for more information.
[3] F. R. Salsbury, Jr. and R. A. Harris, J. Chem. Phys. **107**, 7350 (1997).
[4] F. R. Salsbury, Jr. and R. A. Harris, Chem. Phys. Lett. **279**, 247 (1997).
[5] F. R. Salsbury, Jr. and R. A. Harris, J. Chem. Phys. **108**, 6102 (1998).
[6] A. Olivieri, J. Magn. Reson. **88**, 1 (1990).